JVI Journals.ASM.org

Hepatitis A Virus 3C Protease Cleaves NEMO To Impair Induction of Beta Interferon

Dang Wang,[a] Liurong Fang,[a] Dahai Wei,[b] Huan Zhang,[a] Rui Luo,[a] Huanchun Chen,[a] Kui Li,[b] Shaobo Xiao[a]

State Key Laboratory of Agricultural Microbiology, College of Veterinary Medicine, Huazhong Agricultural University, Wuhan, China[a]; Department of Microbiology, Immunology and Biochemistry, University of Tennessee Health Science Center, Memphis, Tennessee, USA[b]

NEMO (NF-κB essential modulator) is a bridging adaptor indispensable for viral activation of interferon (IFN) antiviral response. Herein, we show that hepatitis A virus (HAV) 3C protease ($3C^{pro}$) cleaves NEMO at the Q304 residue, negating its signaling adaptor function and abrogating viral induction of IFN-β synthesis via the retinoic acid-inducible gene I/melanoma differentiation-associated protein 5 (RIG-I/MDA5) and Toll-like receptor 3 (TLR3) pathways. NEMO cleavage and IFN antagonism, however, were lost upon ablation of the catalytic activity of $3C^{pro}$. These data describe a novel immune evasion mechanism of HAV.

Innate immune responses are activated through host pattern recognition receptors (PRRs), which recognize pathogen-associated molecular patterns (1). Picornaviruses are sensed by retinoic acid-inducible gene I (RIG-I)-like receptors (RLRs), primarily melanoma differentiation-associated protein 5 (MDA5) (2–4) and sometimes RIG-I (5), and by Toll-like receptor 3 (TLR3) (6, 7). Upon engaging viral double-stranded RNAs (dsRNAs), RIG-I and MDA5 recruit mitochondrial antiviral signaling protein (MAVS [also known as IPS-1/VISA/Cardif]), while TLR3 interacts with the Toll–interleukin-1 (IL-1) receptor domain-containing adaptor, inducing interferon beta (IFN-β) (TRIF). Both pathways converge to activate an essential bridging adaptor, NF-κB essential modulator (NEMO), and subsequently classical IKK and IKK-related kinases, leading to phosphorylation of NF-κB and interferon (IFN) regulatory factor 3 (IRF3). These transcription factors directly activate promoters of type I IFNs, such as IFN-β (1).

During its coevolution with humans, hepatitis A virus (HAV), a hepatotropic human picornavirus, has acquired mechanisms to subvert host innate immune responses (8–10). Notably, HAV disrupts RLRs signaling by targeting MAVS for proteolysis by a precursor of its 3C protease ($3C^{Pro}$) cysteine protease, 3ABC (9). HAV also inhibits TLR3 signaling by cleaving TRIF via another precursor, 3CD (10). Herein, we found that mature $3C^{pro}$ inhibited Sendai virus (SEV)-induced IFN-β synthesis by using promoter-based luciferase reporter and enzyme-linked immunosorbent assays (ELISAs) (Fig. 1A and B), demonstrating $3C^{pro}$ is an additional HAV-encoded IFN antagonist. Furthermore, activation of both IRF3-dependent and NF-κB-dependent promoters was dose-dependently impaired by $3C^{pro}$ in human embryonic kidney HEK293T cells, suggesting that $3C^{pro}$ likely targets a step in the IFN-inducing pathway prior to the bifurcation of IRFs and NF-κB (Fig. 1A). Similar results were obtained in human hepatoma Huh7 cells (data not shown).

HAV $3C^{pro}$, as a cysteine proteinase, is responsible for most cleavages within the viral polyprotein (11, 12). To determine whether the protease activity is involved in $3C^{pro}$-mediated IFN-β antagonism, a catalytically deficient $3C^{pro}$ mutant, C172A (13), was examined. In contrast to wild-type (WT) $3C^{pro}$, $3C^{pro}$-C172A was incapable of suppressing SEV-induced IFN-β promoter, implying that $3C^{pro}$ likely proteolytically cleaves a cellular protein(s) to disrupt IFN-β induction (Fig. 1C). Similar results were obtained when cells were transfected with luciferase-tagged IRF3 (IRF3-Luc) or NF-κB-Luc in lieu of IFN-β-Luc (Fig. 1C).

Given the pivotal role of MDA5/RIG-I in sensing of picornaviruses and that RLRs signaling to IRFs and NF-κB diverges at NEMO (14), we investigated whether $3C^{pro}$ targets NEMO or its upstream signaling molecules MAVS, RIG-I, and MDA5 for proteolysis. Compared to an empty plasmid control, overexpression of MDA5, a constitutively active RIG-I mutant (RIG-I-N), MAVS, or a constitutively active NEMO mutant (NEMO-K277A) (15) significantly activated the IFN-β promoter. However, such effects were all significantly reduced upon $3C^{pro}$ coexpression (Fig. 2A), suggesting that $3C^{pro}$ inhibits RLRs signaling at or downstream of NEMO. Interestingly, coexpression of $3C^{pro}$ resulted in marked reduction of ectopically expressed Flag-NEMO, concomitant with the appearance of a faster-migrating band with a molecular mass of ~35 kDa that was detected by an anti-Flag antibody, presumably a $3C^{pro}$ cleavage product (Fig. 2B and C). Importantly, the higher the $3C^{pro}$ expression level, the more ~35-kDa product was expressed while less full-length Flag-NEMO was seen (Fig. 2C). In contrast, no cleavage product was observed for RIG-I, MDA5, or MAVS (Fig. 2B). Remarkably, endogenous NEMO protein was similarly cleaved in $3C^{pro}$-expressing cells (Fig. 2D). The processing intermediates encompassing $3C^{pro}$ (i.e., 3ABC and 3CD) also processed NEMO with the same cleavage pattern as mature $3C^{pro}$, albeit less efficiently than the latter (Fig. 2E). This implies that although these 3C processor forms have evolved unique ability to target MAVS and TRIF, respectively,

Received 27 March 2014 **Accepted** 4 June 2014
Published ahead of print 11 June 2014
Editor: R. M. Sandri-Goldin
Address correspondence to Kui Li, kli1@uthsc.edu, or Shaobo Xiao, vet@mail.hzau.edu.cn.

doi:10.1128/JVI.00869-14

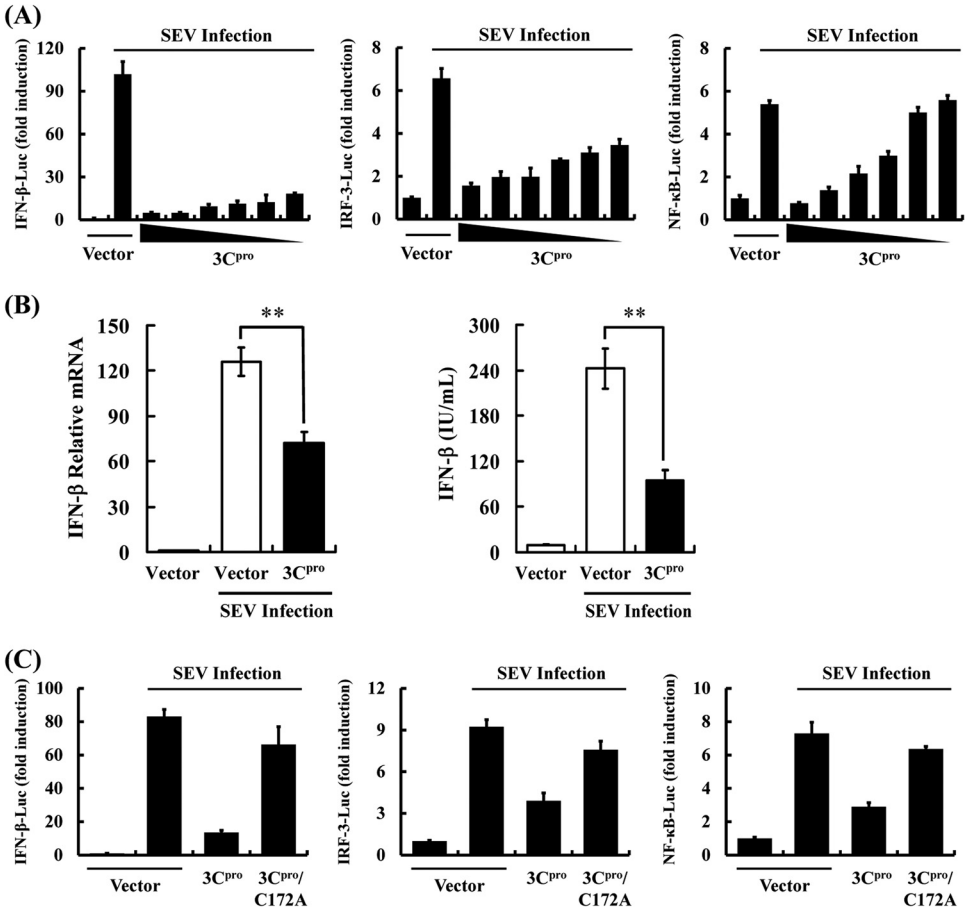

FIG 1 HAV 3C^{pro} inhibits IFN-β promoter activation, and this ability requires the protease activity of 3C^{pro}. (A) HEK293T cells cultured in 24-well plates were transfected with indicated reporter plasmid (0.1 μg), along with pRL-TK (0.02 μg, for normalization of transfection efficiency) plasmid and increasing quantities (0, 0.03125, 0.0625, 0.125, 0.25, 0.5, or 1 μg) of plasmid encoding HAV 3C^{pro}, using Lipofectamine 2000. Twenty-four hours after the initial transfection, the cells were further infected or mock infected with SEV. Luciferase assays were performed 16 h after infection. The results represent the mean and standard deviation from three independent experiments. The firefly luciferase activity was normalized to the *Renilla reniformis* luciferase, and the untreated empty vector control value was set to 1. IFN-β-Luc (left) expresses firefly luciferase under the control of the human IFN-β promoter. 4× IRF3-Luc (middle) and 4× NF-κB-Luc (right) contain four copies of the IRF3- or NF-κB-binding motif in front of a luciferase reporter gene, respectively. (B) HEK293T cells cultured in 24-well plates were transfected with 3C^{pro} expression plasmids or an empty vector (1 μg). Twenty-four hours after initial transfection, cells were further infected or mock infected with SEV. The cells and supernatants were collected at 16 h postinfection and analyzed for IFN-β levels by real-time RT-PCR (left) and ELISA (right). (C) HEK293T cells cultured in 24-well plates were cotransfected with the indicated reporter plasmid, along with pRL-TK plasmid and the designated 3C^{pro} expression plasmids (1 μg). An empty vector was used as a control. Twenty-four hours after initial transfection, cells were further infected or mock infected with SEV. Luciferase assays were performed 16 h after infection.

they share with mature 3C^{pro} the capacity to hydrolyze NEMO. Note that ectopic expression of 3CD was less effective in cleaving NEMO than overexpression of 3C^{pro}, although it produced a comparable amount of mature 3C^{pro} to the latter. 3D or 3CD could form a complex with 3C^{pro} matured from 3CD (16–18) impairing the proteolytic activity of 3C^{pro} toward NEMO. Importantly, 3C^{pro}-induced cleavage of NEMO was independent of cellular caspases or the proteasome, as not reversed by treatment with ZVAD or MG132 (Fig. 2F). Confirming that 3C^{pro} produced in the context of virus infection is capable of NEMO cleavage, we found that the protein abundance of both ectopically expressed Flag-NEMO and endogenous NEMO was substantially reduced in HAV-infected HEK293T cells (Fig. 2G). In these experiments, the degree of NEMO reduction correlated with the HAV infection dose, and substantial NEMO degradation coincided with a high level of HAV RNA replication at 36 h postinfection and beyond (Fig. 2G). We also observed that the level of endogenous NEMO protein is higher than that of ectopically expressed Flag-NEMO (data not shown). This could explain why HAV infection appeared to degrade Flag-NEMO more efficiently that it did endogenous NEMO. Consistent with the fact that NEMO is required for activation of the IFN response downstream of both RLRs and TLR3 pathways, extracellular dsRNA [poly(I·C)]-induced activation of the IFN-β promoter in 293-TLR3 cells was blunted by 3C^{pro} (Fig. 2H).

Since WT NEMO did not significantly activate IRFs and NF-κB to induce IFN-β (19), we used a constitutively active NEMO mutant, NEMO-K277A, to examine the effect of 3C^{pro}-mediated NEMO cleavage on IFN-β induction. NEMO-K277A remained susceptible to WT 3C^{pro} cleavage but not to the C172A mutant (Fig. 3A and B). As a result, overexpression of

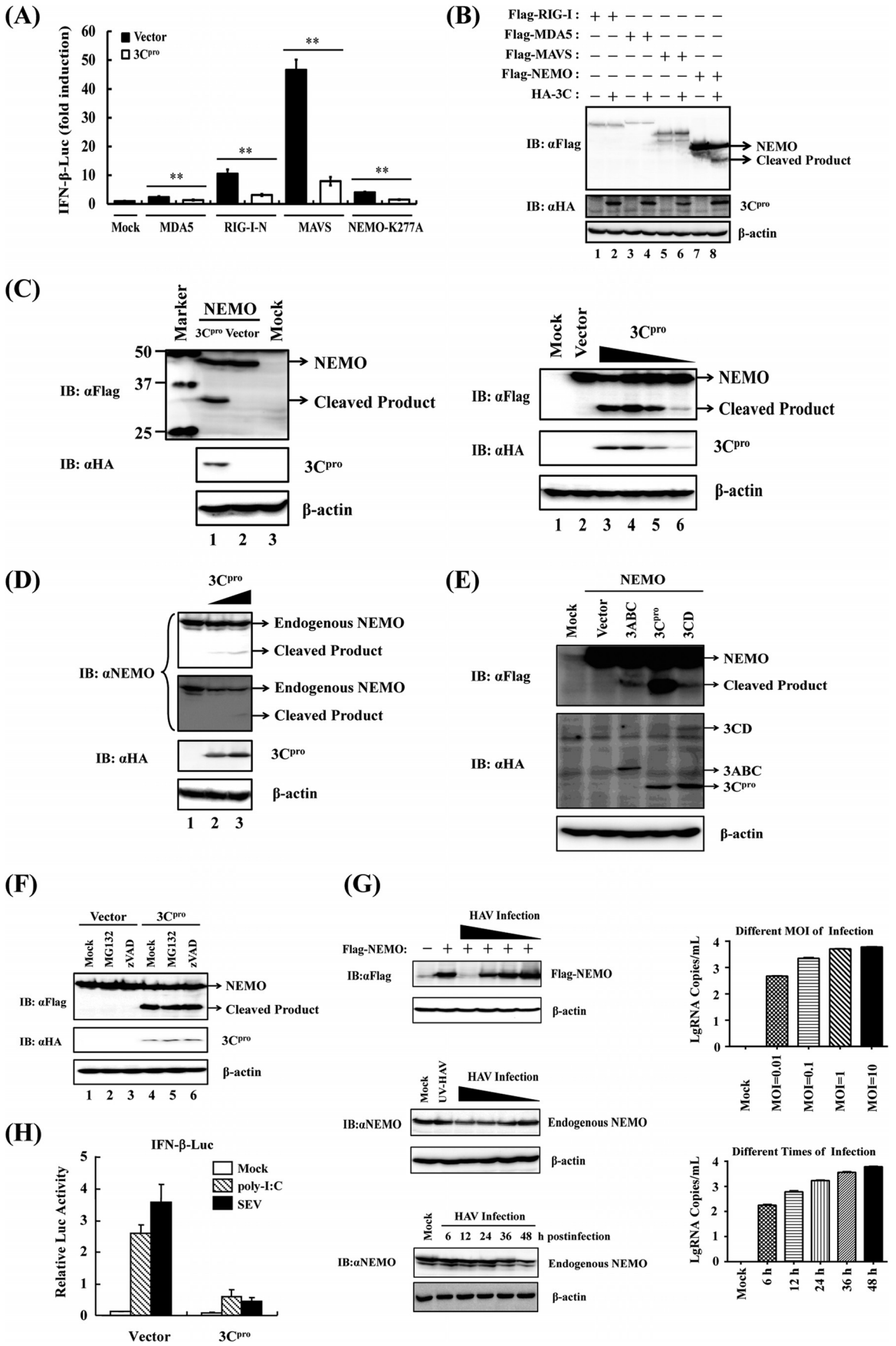
(A)
IFN-β-Luc (fold induction)
Vector
3Cpro
Mock
MDA5
RIG-I-N
MAVS
NEMO-K277A
(B)
Flag-RIG-I :
Flag-MDA5 :
Flag-MAVS :
Flag-NEMO :
HA-3C :
IB: αFlag
IB: αHA
NEMO
Cleaved Product
3Cpro
β-actin
(C)
Marker
NEMO
3Cpro Vector
Mock
IB: αFlag
IB: αHA
(D)
3Cpro
IB: αNEMO
Endogenous NEMO
Cleaved Product
(E)
Mock
Vector
3ABC
3CD
(F)
MG132
zVAD
(G)
HAV Infection
Flag-NEMO:
IB:αFlag
IB:αNEMO
UV-HAV
6 12 24 36 48 h postinfection
Different MOI of Infection
LgRNA Copies/mL
MOI=0.01
MOI=0.1
MOI=1
MOI=10
Different Times of Infection
6 h
12 h
24 h
36 h
48 h
(H)
IFN-β-Luc
Relative Luc Activity
poly-I:C
SEV

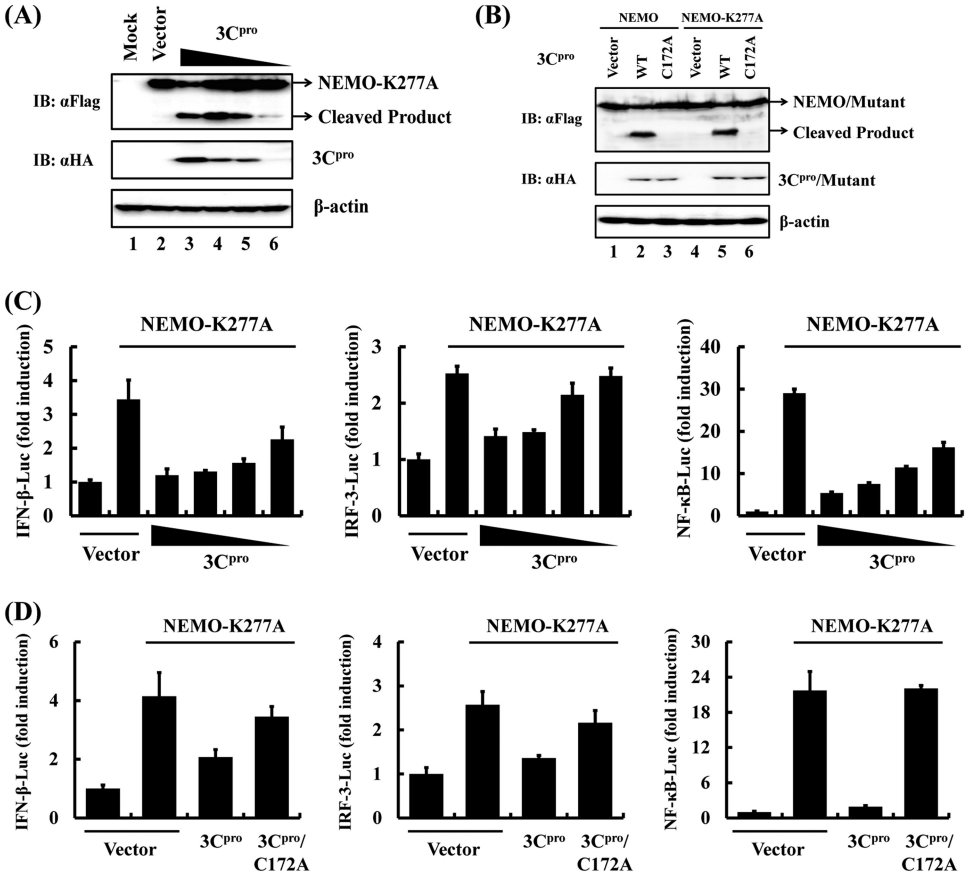

FIG 3 HAV 3C^{pro} disrupts NEMO-mediated IFN-β induction. (A) HEK293T cells cultured in 60-mm dishes were transfected with Flag-tagged NEMO-K277A expression plasmid (2 μg) along with plasmid encoding HA-tagged 3C^{pro} (1 μg). Cell lysates were prepared 30 h posttransfection and analyzed by Western blotting. (B) HEK293T cells cultured in 60-mm dishes were transfected with Flag-tagged NEMO expression plasmid (2 μg), along with the indicated 3C^{pro} expression plasmids (1 μg). Cell lysates were prepared 30 h posttransfection and analyzed by Western blotting. (C) HEK293T cells cultured in 24-well plates were transfected with the indicated reporter plasmid (0.1 μg), pRL-TK (0.02 μg), and Flag-tagged NEMO-K277A expression plasmid (0.5 μg), along with increasing quantities (0, 0.0625, 0.125, 0.25, or 0.5 μg) of plasmid encoding 3C^{pro}. Luciferase assays were performed at 36 h after the transfection. (D) HEK293T cells cultured in 24-well plates were cotransfected with the indicated reporter plasmid, pRL-TK plasmid, and Flag-tagged NEMO-K277A expression plasmid (0.5 μg) along with the designated 3C^{pro} expression plasmids (0.5 μg). An empty vector (pCMV-HA) was used as a control. Cell extracts were collected 36 h after transfection and analyzed for firefly and *Renilla* luciferase expression.

FIG 2 HAV 3C^{pro} disrupts RLR signaling by cleaving NEMO. (A) HEK293T cells cultured in 24-well plates were cotransfected with IFN-β-Luc, pRL-TK plasmid, and plasmid encoding 3C^{pro} (0.3 μg), together with the MDA5, RIG-I-N, MAVS, or NEMO-K277A expression vector (0.7 μg). Luciferase assays were performed 36 h after transfection. **, $P < 0.01$ (considered highly significant). (B) HEK293T cells cultured in 60-mm-diameter dishes were transfected with Flag-tagged RIG-I, MDA5, MAVS, or NEMO expression plasmid (4 μg) along with empty vector or plasmid encoding hemagglutinin (HA)-tagged 3C^{pro} (0.5 μg). Cell lysates were prepared 30 h posttransfection and analyzed by Western blotting (immunoblotting [IB]). (C) (Left) HEK293T cells cultured in 60-mm-diameter dishes were transfected with Flag-tagged NEMO expression plasmid (2 μg) along with empty vector or plasmid encoding HA-tagged 3C^{pro} (1 μg). Cell lysates were prepared 30 h posttransfection and analyzed by Western blotting. The lane with protein markers (Bio-Rad, catalog no. 161-0376) includes 50-, 37-, and 25-kDa molecular mass bands. (Right) HEK293T cells cultured in 60-mm dishes were transfected with Flag-tagged NEMO expression plasmid (2 μg), along with increasing quantities (0, 0.125, 0.25, 0.5, or 1 μg) of plasmid encoding HA-tagged 3C^{pro}. Cell lysates were prepared 30 h posttransfection and analyzed by Western blotting. (D) HEK293T cells cultured in 60-mm dishes were transfected with increasing quantities (0, 2, or 4 μg) of plasmid encoding HA-tagged 3C^{pro}. Cells were lysed 30 h posttransfection and analyzed by Western blotting. (Two different exposures of the blot are shown.) (E) HEK293T cells cultured in 60-mm dishes were transfected with Flag-tagged wild-type NEMO as indicated (2 μg), along with HA-3C^{pro} or 3C^{pro}-containing precursors (1 μg). Cell lysates were prepared 30 h posttransfection and analyzed by Western blotting. (F) HEK293T cells cultured in 60-mm dishes were cotransfected with Flag-tagged NEMO expression plasmid (2 μg) and plasmid encoding 3C^{pro} or empty vector (1 μg). Twenty-four hours after transfection, MG132 or zVAD-FMK was added to a final concentration of 20 μM. Cell lysates were prepared 8 h after treatment and analyzed by Western blotting. (G) (Top) HEK293T cells cultured in 60-mm dishes were transfected with Flag-tagged NEMO (Flag-NEMO) and infected with different doses (multiplicities of infection [MOI] of 0.01, 0.1, 1, and 10) of HAV (L-A-1 attenuated vaccine strain) 6 h posttransfection. The cells were lysed 36 h postinfection and analyzed by Western blotting. (Middle) HEK293T cells were infected with different doses of HAV or, as a control, UV light-inactivated HAV (UV-HAV). The cells were lysed 36 h postinfection and analyzed by Western blotting. (Bottom) HEK293T cells were infected with HAV (MOI of 1), lysed at different times of HAV postinfection, and analyzed by Western blotting. Expression of Flag-NEMO conjugated protein and endogenous NEMO protein was verified by mouse anti-Flag antibody (Macgene, China) or rabbit anti-NEMO (Abclonal, China), respectively. Mouse anti-HA (Abclonal, China) was used to confirm the expression of 3C^{pro}, and mouse anti-β-actin antibody (Beyotime, China) was used to detect β-actin, which serves as a protein loading control. (H) Activation of the IFN-β promoter by extracellular poly(I·C) (20 μg/ml) or SEV (100 hemagglutinating units [HAU]/ml) in HEK293-TLR3 cells transiently expressing 3C^{pro} or a control vector.

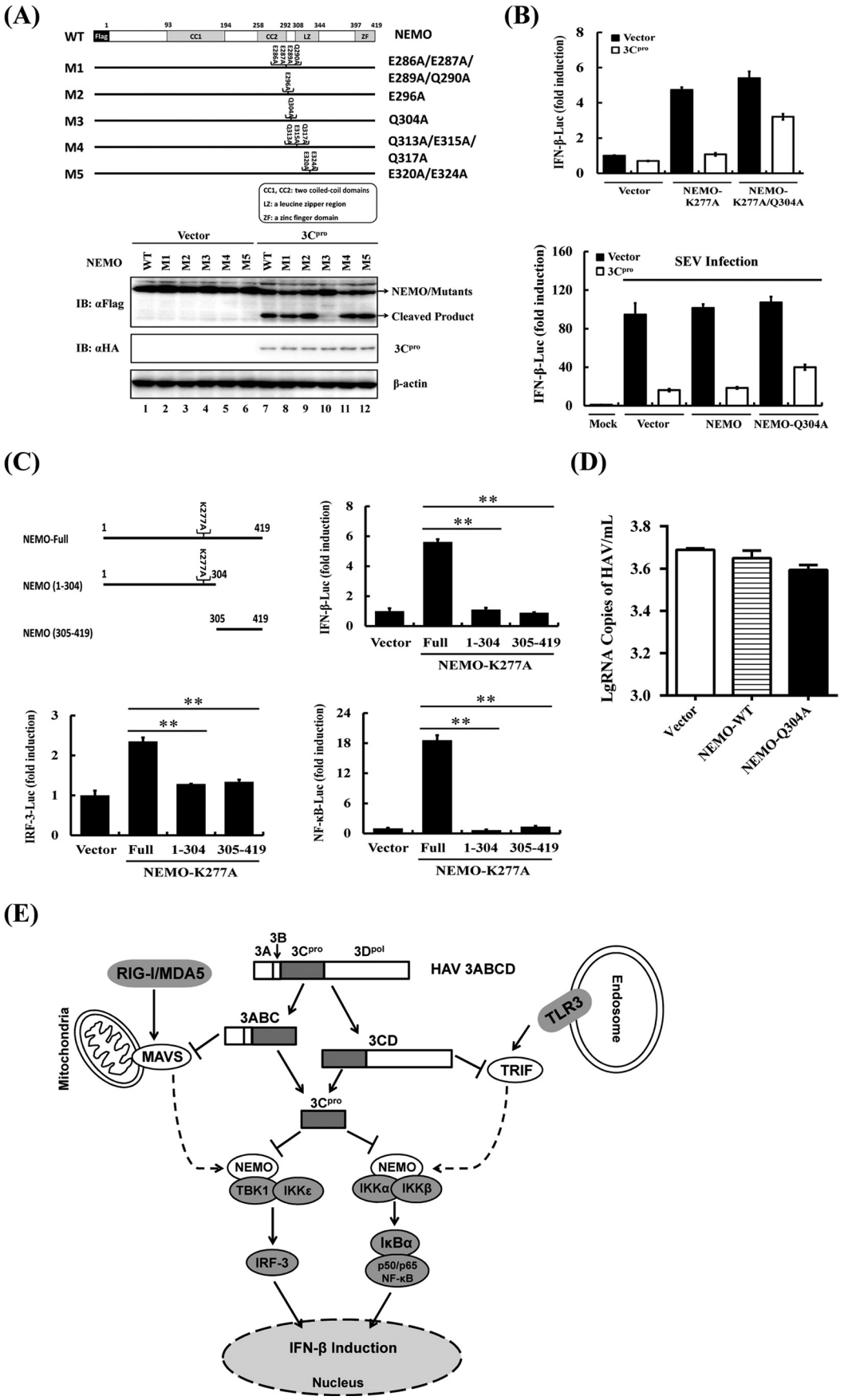
(A)
WT
M1
M2
M3
M4
M5
NEMO
E286A/E287A/ E289A/Q290A
E296A
Q304A
Q313A/E315A/ Q317A
E320A/E324A
CC1, CC2: two coiled-coil domains
LZ: a leucine zipper region
ZF: a zinc finger domain
Vector
3Cpro
IB: αFlag
IB: αHA
β-actin
NEMO/Mutants
Cleaved Product
(B)
IFN-β-Luc (fold induction)
Vector
NEMO-K277A
NEMO-K277A/Q304A
SEV Infection
Mock
NEMO
NEMO-Q304A
(C)
NEMO-Full
NEMO (1-304)
NEMO (305-419)
IRF-3-Luc (fold induction)
NF-κB-Luc (fold induction)
Full
1-304
305-419
NEMO-K277A
(D)
LgRNA Copies of HAV/mL
NEMO-WT
(E)
RIG-I/MDA5
MAVS
Mitochondria
3A
3B
3Cpro
3Dpol
HAV 3ABCD
3ABC
3CD
TLR3
Endosome
TRIF
NEMO
TBK1
IKKε
IKKα
IKKβ
IRF-3
IκBα
p50/p65 NF-κB
IFN-β Induction
Nucleus

3C^{pro} dose-dependently inhibited NEMO-K277A-mediated IFN-β promoter activation by disrupting activation of IRF3 and NF-κB (Fig. 3C). In contrast, the catalytically inactive 3C^{pro}-C172A mutant was without effect (Fig. 3D), consistent with the inability of 3C^{pro}-C172A to cleave NEMO (or NEMO-K277A) (Fig. 3B).

Because NEMO cleavage produced an ~35-kDa product and the 3C^{pro} substrate specificity documented a preference for glutamine (Gln [Q]) or glutamic acid (Glu [E]) at the P1 position (20), we examined the sequence of NEMO for potential 3C^{pro} cleavage sites that could potentially generate fragments of the appropriate size following 3C^{pro} scission and constructed a cluster of NEMO mutants in which the invariant Gln or Glu at each potential P1 position was replaced with alanine (Ala [A]) (Fig. 4A, upper panel). 3C^{pro}-mediated NEMO cleavage was not affected by E286A E287A E289A Q290A, E296A, Q313A E315A Q317A, or E320A E324A mutations. In contrast, the Q304A substitution blocked the appearance of the cleavage product as well as the reduction in abundance of full-length NEMO (Fig. 4A, lower panel, lane 10), suggesting 3C^{pro} cleaved NEMO at Gln304. As further evidence supporting this notion, the Q304A mutation also rendered NEMO-K277A resistant to 3C^{pro} cleavage (data not shown). We found that the constitutively active NEMO-K277A bearing the Q304A mutation significantly overcame the 3C^{pro} blockade on activation of the IFN-β promoter compared with its 3C^{pro}-sensitive counterpart (Fig. 4B). Furthermore, ectopic expression of NEMO-Q304A, but not WT NEMO, substantially restored Sendai virus-induced IFN-β promoter activity (Fig. 4B). The incomplete restoration of IFN activation by the Q304A mutant NEMO could be attributed to the ability of HAV 3C^{pro} to associate with NEMO and inhibit assembly of NEMO-containing signaling complexes, in addition to NEMO cleavage, as has been observed with foot-and-mouth-disease virus 3C^{pro} (19). This possibility needs to be investigated in future studies.

To further determine whether either of the 3C^{pro}-induced cleavage fragments of NEMO would remain active, we ectopically expressed the constitutively active NEMO-K277A, the N-terminal fragment of NEMO-K277A (residues 1 to 304), or the C-terminal fragment of NEMO (residues 305 to 419) that would result from 3C^{pro} cleavage and examined their abilities to activate IFN-β and IRF3/NF-κB-dependent promoters. In contrast to full-length NEMO-K277A which was competent in inducing all 3 promoters, neither the N-terminal nor C-terminal fragment retained such abilities (Fig. 4C), suggesting that 3C^{pro}-mediated cleavage of NEMO efficiently inactivates NEMO-mediated downstream signaling. In addition, reconstitution of NEMO signaling by the Q304A mutant NEMO led to a modest reduction (~20%) in HAV replication (Fig. 4D) as revealed by quantitative reverse transcription-PCR (RT-qPCR) (21).

In summary, our data identify 3C^{pro} as a novel IFN antagonist encoded by HAV and show that the 3C^{pro}-mediated proteolytic cleavage of NEMO is directly involved in inhibition of IFN-β transcription. By virtue of this, our study describes a novel mechanism by which HAV counteracts the host's innate antiviral responses. The multipronged targeting of MAVS, TRIF, and NEMO by HAV through 3ABC, 3CD, and 3C^{pro} illustrates a remarkable example of picornaviral evolution, disarming host innate immunity to the greatest extent possible and offering the virus a maximal survival advantage (Fig. 4E). This also could explain the striking observation that acute HAV infection is associated with a very limited type I IFN response, despite the persistence of intrahepatic viral RNA (8). Previously, we reported that NEMO is a substrate for 3C^{pro} of another picornavirus, foot-and-mouth disease virus (19). Recently, 3C^{pro} of enterovirus 71 was reported to target interferon regulatory factor 7 (IRF7) for proteolysis (22). We did not find this viral protease to cleave NEMO (data not shown), indicating that targeting NEMO for immune evasion is adopted by some but not all picornaviruses. Exactly how the differential targeting of NEMO affects innate immune responses and/or picornaviral pathogenesis *in vivo* will require further study.

ACKNOWLEDGMENTS

This research was supported by the National Natural Sciences Foundation of China (31225027 and 31121004), the National Basic Research Program (973) of China (2014CB522700), the Fundamental Research Funds for the Central Universities (2013PY043), and the U.S. National Institutes of Health (AI069285).

REFERENCES

1. **Kawai T, Akira S.** 2006. Innate immune recognition of viral infection. Nat. Immunol. **7:**131–137. http://dx.doi.org/10.1038/ni1303.
2. **Gitlin L, Barchet W, Gilfillan S, Cella M, Beutler B, Flavell RA, Diamond MS, Colonna M.** 2006. Essential role of mda-5 in type I IFN responses to polyriboinosinic:polyribocytidylic acid and encephalomyocarditis picornavirus. Proc. Natl. Acad. Sci. U. S. A. **103:**8459–8464. http://dx.doi.org/10.1073/pnas.0603082103.
3. **Husser L, Alves MP, Ruggli N, Summerfield A.** 2011. Identification of the role of RIG-I, MDA-5 and TLR3 in sensing RNA viruses in porcine epithelial cells using lentivirus-driven RNA interference. Virus Res. **159:**9–16. http://dx.doi.org/10.1016/j.virusres.2011.04.005.

FIG 4 HAV 3C^{pro}-mediated NEMO cleavage is involved in the inhibition of IFN-β induction. (A) Schematic representation of wild-type NEMO and its derivatives (top). HEK293T cells cultured in 60-mm-diameter dishes were transfected with Flag-tagged wild-type NEMO or NEMO mutants as indicated, along with HA-3C^{pro} or empty vector. Cell lysates were prepared 30 h posttransfection and analyzed by Western blotting. (B) HEK293T cells cultured in 24-well plates were cotransfected with IFN-β-Luc, pRL-TK plasmid, and plasmid encoding 3C^{pro} (0.3 μg) together with the empty vector, NEMO-K277A, or the NEMO-K277A/Q304A expression vector (0.7 μg). Luciferase assays were performed 36 h after transfection (top). HEK293T cells cultured in 24-well plates were cotransfected with IFN-β-Luc, pRL-TK plasmid, and plasmid encoding 3C^{pro} (0.3 μg) together with the empty vector, NEMO, or the NEMO-Q304A expression vector (0.7 μg). Twenty-four hours after the initial transfection, the cells were further infected or mock infected with SEV. Luciferase assays were performed at 16 h after infection (down). (C) HEK293T cells cultured in 24-well plates were cotransfected with IFN-β-Luc, pRL-TK plasmid and either 1 μg of plasmid encoding Flag-fused NEMO-K277A (Full), putative 3C^{pro}-induced cleavage fragments of NEMO-K277A, or empty vector. Cell extracts were collected 36 h after transfection and analyzed for firefly and *Renilla* luciferase expression. **, $P < 0.01$ (considered highly significant). (D) HEK293T cells cultured in 24-well plates were transfected with the indicated NEMO-expressing plasmids and infected with HAV (L-A-1 attenuated vaccine strain; MOI of 1) 12 h posttransfection. The cells were lysed 36 h postinfection and analyzed by RT-qPCR according to the reference methods (21). (E) Type I interferon signaling pathways disrupted by HAV 3C^{pro} and its precursors. HAV 3C^{pro} and its processing intermediates disrupt IFN-β induction by 3ABC-mediated proteolysis of MAVS (9), 3CD-mediated proteolysis of TRIF (10), and 3C^{pro}-mediated proteolysis of NEMO in this study.

4. **Kato H, Takeuchi O, Sato S, Yoneyama M, Yamamoto M, Matsui K, Uematsu S, Jung A, Kawai T, Ishii KJ, Yamaguchi O, Otsu K, Tsujimura T, Koh CS, Reis e Sousa C, Matsuura Y, Fujita T, Akira S.** 2006. Differential roles of MDA5 and RIG-I helicases in the recognition of RNA viruses. Nature **441:**101–105. http://dx.doi.org/10.1038/nature04734.
5. **Papon L, Oteiza A, Imaizumi T, Kato H, Brocchi E, Lawson TG, Akira S, Mechti N.** 2009. The viral RNA recognition sensor RIG-I is degraded during encephalomyocarditis virus (EMCV) infection. Virology **393:**311–318. http://dx.doi.org/10.1016/j.virol.2009.08.009.
6. **Oshiumi H, Okamoto M, Fujii K, Kawanishi T, Matsumoto M, Koike S, Seya T.** 2011. The TLR3/TICAM-1 pathway is mandatory for innate immune responses to poliovirus infection. J. Immunol. **187:**5320–5327. http://dx.doi.org/10.4049/jimmunol.1101503.
7. **Negishi H, Osawa T, Ogami K, Ouyang X, Sakaguchi S, Koshiba R, Yanai H, Seko Y, Shitara H, Bishop K, Yonekawa H, Tamura T, Kaisho T, Taya C, Taniguchi T, Honda K.** 2008. A critical link between Toll-like receptor 3 and type II interferon signaling pathways in antiviral innate immunity. Proc. Natl. Acad. Sci. U. S. A. **105:**20446–20451. http://dx.doi.org/10.1073/pnas.0810372105.
8. **Lanford RE, Feng Z, Chavez D, Guerra B, Brasky KM, Zhou Y, Yamane D, Perelson AS, Walker CM, Lemon SM.** 2011. Acute hepatitis A virus infection is associated with a limited type I interferon response and persistence of intrahepatic viral RNA. Proc. Natl. Acad. Sci. U. S. A. **108:**11223–11228. http://dx.doi.org/10.1073/pnas.1101939108.
9. **Yang Y, Liang Y, Qu L, Chen Z, Yi M, Li K, Lemon SM.** 2007. Disruption of innate immunity due to mitochondrial targeting of a picornaviral protease precursor. Proc. Natl. Acad. Sci. U. S. A. **104:**7253–7258. http://dx.doi.org/10.1073/pnas.0611506104.
10. **Qu L, Feng Z, Yamane D, Liang Y, Lanford RE, Li K, Lemon SM.** 2011. Disruption of TLR3 signaling due to cleavage of TRIF by the hepatitis A virus protease-polymerase processing intermediate, 3CD. PLoS Pathog. **7:**e1002169. http://dx.doi.org/10.1371/journal.ppat.1002169.
11. **Schultheiss T, Kusov YY, Gauss-Muller V.** 1994. Proteinase 3C of hepatitis A virus (HAV) cleaves the HAV polyprotein P2-P3 at all sites including VP1/2A and 2A/2B. Virology **198:**275–281. http://dx.doi.org/10.1006/viro.1994.1030.
12. **Schultheiss T, Sommergruber W, Kusov Y, Gauss-Muller V.** 1995. Cleavage specificity of purified recombinant hepatitis A virus 3C proteinase on natural substrates. J. Virol. **69:**1727–1733.
13. **Bergmann EM, Mosimann SC, Chernaia MM, Malcolm BA, James MN.** 1997. The refined crystal structure of the 3C gene product from hepatitis A virus: specific proteinase activity and RNA recognition. J. Virol. **71:**2436–2448.
14. **Zhao T, Yang L, Sun Q, Arguello M, Ballard DW, Hiscott J, Lin R.** 2007. The NEMO adaptor bridges the nuclear factor-kappaB and interferon regulatory factor signaling pathways. Nat. Immunol. **8:**592–600. http://dx.doi.org/10.1038/ni1465.
15. **Bloor S, Ryzhakov G, Wagner S, Butler PJ, Smith DL, Krumbach R, Dikic I, Randow F.** 2008. Signal processing by its coil zipper domain activates IKK gamma. Proc. Natl. Acad. Sci. U. S. A. **105:**1279–1284. http://dx.doi.org/10.1073/pnas.0706552105.
16. **Zell R, Seitz S, Henke A, Munder T, Wutzler P.** 2005. Linkage map of protein-protein interactions of porcine teschovirus. J. Gen. Virol. **86:**2763–2768. http://dx.doi.org/10.1099/vir.0.81144-0.
17. **Shen M, Reitman ZJ, Zhao Y, Moustafa I, Wang Q, Arnold JJ, Pathak HB, Cameron CE.** 2008. Picornavirus genome replication. Identification of the surface of the poliovirus (PV) 3C dimer that interacts with PV 3Dpol during VPg uridylylation and construction of a structural model for the PV 3C2-3Dpol complex. J. Biol. Chem. **283:**875–888. http://dx.doi.org/10.1074/jbc.M707907200.
18. **Pathak HB, Arnold JJ, Wiegand PN, Hargittai MR, Cameron CE.** 2007. Picornavirus genome replication: assembly and organization of the VPg uridylylation ribonucleoprotein (initiation) complex. J. Biol. Chem. **282:**16202–16213. http://dx.doi.org/10.1074/jbc.M610608200.
19. **Wang D, Fang L, Li K, Zhong H, Fan J, Ouyang C, Zhang H, Duan E, Luo R, Zhang Z, Liu X, Chen H, Xiao S.** 2012. Foot-and-mouth disease virus 3C protease cleaves NEMO to impair innate immune signaling. J. Virol. **86:**9311–9322. http://dx.doi.org/10.1128/JVI.00722-12.
20. **Seipelt J, Guarne A, Bergmann E, James M, Sommergruber W, Fita I, Skern T.** 1999. The structures of picornaviral proteinases. Virus Res. **62:**159–168. http://dx.doi.org/10.1016/S0168-1702(99)00043-X.
21. **Qiu F, Zheng H, Yi Y, Jia Z, Cao J, Bi S.** 2013. Comparative evaluation of a novel TaqMan real-time reverse transcription-polymerase chain reaction assay for hepatitis A virus detection. J. Int. Med. Res. **41:**427–434. http://dx.doi.org/10.1177/0300060513476434.
22. **Lei X, Xiao X, Xue Q, Jin Q, He B, Wang J.** 2013. Cleavage of interferon regulatory factor 7 by enterovirus 71 3C suppresses cellular responses. J. Virol. **87:**1690–1698. http://dx.doi.org/10.1128/JVI.01855-12.